

## Liquid-State Nuclear Spin Comagnetometers

M. P. Ledbetter,<sup>1,\*</sup> S. Pustelny,<sup>1,2</sup> D. Budker,<sup>1,3</sup> M. V. Romalis,<sup>4</sup> J. W. Blanchard,<sup>5</sup> and A. Pines<sup>5,6</sup>

<sup>1</sup>*Department of Physics, University of California at Berkeley, Berkeley, California 94720-7300, USA*

<sup>2</sup>*Center for Magneto-Optical Research, Institute of Physics, Jagiellonian University, Reymonta 4, PL-30-059 Kraków, Poland*

<sup>3</sup>*Nuclear Science Division, Lawrence Berkeley National Laboratory, Berkeley, California 94720, USA*

<sup>4</sup>*Department of Physics, Princeton University, Princeton, New Jersey 08544, USA*

<sup>5</sup>*Department of Chemistry, University of California at Berkeley, Berkeley, California 94720-3220, USA*

<sup>6</sup>*Materials Science Division, Lawrence Berkeley National Laboratory, Berkeley, California 94720, USA*

(Received 19 February 2012; published 15 June 2012)

We discuss nuclear spin comagnetometers based on ultralow-field nuclear magnetic resonance in mixtures of miscible solvents, each rich in a different nuclear spin. In one version thereof, Larmor precession of protons and  $^{19}\text{F}$  nuclei in a mixture of thermally polarized pentane and hexafluorobenzene is monitored via a sensitive alkali-vapor magnetometer. We realize transverse relaxation times in excess of 20 s and suppression of magnetic field fluctuations by a factor of 3400. We estimate it should be possible to achieve single-shot sensitivity of about  $5 \times 10^{-9}$  Hz, or about  $5 \times 10^{-11}$  Hz in  $\approx 1$  day of integration. In a second version, spin precession of protons and  $^{129}\text{Xe}$  nuclei in a mixture of pentane and hyperpolarized liquid xenon is monitored using superconducting quantum interference devices. Application to spin-gravity experiments, electric dipole moment experiments, and sensitive gyroscopes is discussed.

DOI: [10.1103/PhysRevLett.108.243001](https://doi.org/10.1103/PhysRevLett.108.243001)

PACS numbers: 07.55.Ge, 11.30.Er, 31.30.jn, 33.25.+k

Atomic comagnetometers based on overlapping ensembles of different spins form the basis for experimental tests of spin-gravity coupling [1], searches for permanent electric dipole moments (EDMs) [2–4], tests of Lorentz and *CPT* violation [5–7], and sensitive gyroscopes [8]. In searches for exotic interactions in which one is looking for a Zeeman-like interaction, the precession frequency of one species can be used to compensate for magnetic field noise. Most such devices employ spins in gas-phase systems. Here we demonstrate a new class of comagnetometers based on overlapping ensembles of nuclear spins in liquid state. The technique has the potential to strengthen limits on spin-gravity coupling and EDMs by several orders of magnitude. Application to inertial sensing is also discussed.

Our technique is based on ultralow-field nuclear magnetic resonance of binary mixtures of mutually miscible solvents, each rich in a different nuclear spin species. Rather than using inductive pickup coils, as in traditional proton-precession magnetometers [9–11], we use sensitive alkali-vapor or superconducting quantum interference device (SQUID) magnetometers to probe nuclear spin precession, enabling measurements to be performed with high signal-to-noise ratio at low magnetic fields ( $\approx 1$  mG) suitable for precision measurements. Our discussion is primarily focused on a proton- $^{19}\text{F}$  comagnetometer in a mixture of pentane and hexafluorobenzene (HFB), in which spins are thermally prepolarized in a strong magnetic field. Spin precession is then monitored via an alkali-vapor magnetometer in a  $\approx 1$  mG field. We realize  $T_2^*$  of 13.7 and 20.8 s for  $^1\text{H}$  and  $^{19}\text{F}$ , respectively. Based on signal-to-noise projections for realistic conditions, we

estimate that frequency resolution of about  $5 \times 10^{-9}$  Hz can be achieved in a single shot, or about  $10^{-11}$  Hz in approximately 1 day of integration. Sensitivity limits imposed by spin-projection noise are several orders of magnitude smaller.

We also briefly mention operation of a proton- $^{129}\text{Xe}$  comagnetometer using a mixture of hyperpolarized liquid xenon and pentane. In this version, SQUIDs are used to monitor nuclear spin precession in 10 mG magnetic fields. In the Xe-pentane comagnetometer,  $T_2$  is 3.5 and  $\approx 250$  s for  $^1\text{H}$  and  $^{129}\text{Xe}$ , respectively.

The experimental setup used for the pentane-HFB comagnetometer is similar to that of Ref. [12] and is discussed in the Supplemental Material [13]. Very briefly, solvent mixtures (roughly 100  $\mu\text{L}$ ) were degassed via five freeze-thaw cycles under vacuum and flame sealed in a 5 mm nuclear magnetic resonance (NMR) tube. Samples were thermally polarized in a 20 kG magnet and pneumatically shuttled into a low-field ( $B_z \approx 1$  mG) detection region adjacent to an alkali-vapor atomic magnetometer, which is sensitive to magnetic fields in the transverse direction. A small “guiding field” ( $\approx 100$  mG) was applied in the  $x$  direction during transit, and then abruptly removed prior to signal acquisition, so that the initial spin magnetization is in the  $x$  direction.

Figure 1 shows the single-shot ultralow-field NMR signal obtained in a mixture of pentane and HFB (roughly equal volumes). The signal is well described by a sum of two exponentially decaying sinusoids, with transverse relaxation time  $T_2^* = 13.7$  and 20.8 s for protons and  $^{19}\text{F}$  nuclei, respectively. Obtaining such long transverse relaxation times required careful compensation of magnetic field

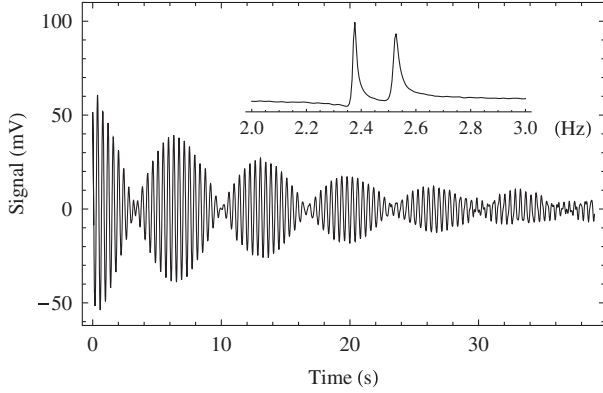


FIG. 1. Ultralow-field (0.6 mG) NMR signal (single shot) from a mixture of pentane and hexafluorobenzene. Data are well described by the sum of two exponentially decaying sinusoids with  $T_2^* = 13.7$  and 20.8 s. The inset shows the real part of the Fourier transform.

gradients. Uncertainties in the frequencies extracted from the fit are typically on the order of 30–70  $\mu\text{Hz}$ . The inset in Fig. 1 shows the real part of the Fourier transform. The mixed phase of the signal is because the precessing nuclei produce magnetic fields in both the  $x$  and  $y$  directions with sinusoidal and cosinusoidal dependence, respectively. In the presence of  $B_z$ , the alkali-vapor magnetometer signal is due to a linear combination of both components. The observed phase is in agreement with auxiliary calibrations, and is discussed in more depth in the Supplemental Material [13]. Similar signals were also obtained in a mixture of HFB and acetone (see Supplemental Material [13]).

It is worth noting that neat cyclopentane had  $T_2^* = 11$  s (probably limited by gradients) and neat benzene had  $T_2^* = 21$  s (after optimizing gradients); however, mixtures of hexafluorobenzene and cyclopentane or benzene yielded fast relaxation, with  $T_2 \approx 0.8$  s. This may be due to strong intermolecular interactions between benzene and HFB [14], or possibly due to residual oxygen. For reference, signals from neat pentane, cyclopentane, benzene, tetramethylsilane, and  $^{13}\text{C}$  labeled formic acid are presented in the Supplemental Material [13].

As a demonstration of operation as a comagnetometer, we present in Fig. 2(a) the frequency of  $^1\text{H}$  and  $^{19}\text{F}$  nuclei in a mixture of pentane and HFB for 32 transients. The magnetic field was switched between  $B_z = B_0 \pm 3.7 \mu\text{G}$  in between transients ( $B_0 = 950 \mu\text{G}$ ), corresponding to a peak-to-peak modulation of about 1 part in 120. The two frequencies track each other well. To characterize the degree to which magnetic field fluctuations may be compensated, we plot the ratio  $\nu_f/\nu_h$  in Fig. 2(b), where there is no apparent modulation. Peak-to-peak amplitude of  $\nu_f/\nu_h$  at the magnetic field modulation frequency (determined using a software lock-in) is at the level of 1 part in 420 000, representing suppression of magnetic field noise by a factor of about 3400.

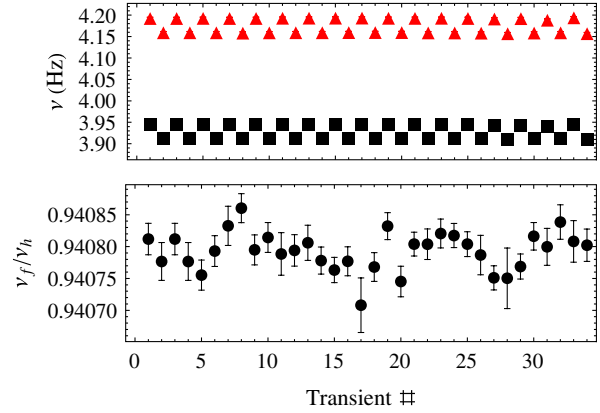


FIG. 2 (color online). Demonstration of the operation as a comagnetometer. (a) Free precession frequency of  $^1\text{H}$  (triangles) and  $^{19}\text{F}$  (squares) nuclei is shown as a small modulation is applied to  $B_z$ ,  $\Delta B_z \approx 3.7 \mu\text{G}$ , demonstrating that the two frequencies track each other closely. (b) Modulation is not visible in the ratio  $\nu_f/\nu_h$ .

The data in Fig. 2(b) are consistent with literature values for the magnetic moments of protons and  $^{19}\text{F}$  [15], which give  $\nu_f/\nu_h = 0.94077$ ; however, they display long term drift in the ratio that is somewhat larger than the errors in individual measurements. A likely explanation for this is spin-density gradients in the vertical ( $x$ ) direction due to thermodiffusion in the presence of temperature gradients across the sample. We experimentally confirm a small vertical separation  $\Delta$  between the “centers of spin” by examining the dependence of  $\nu_f/\nu_h$  on the gradient  $g_x = dB_z/dx$  (Fig. 3). We find that  $\nu_f/\nu_h$  is roughly linear in the gradient, with a slope  $-8.8 \times 10^{-6} \text{ cm}/\mu\text{G}$ . To first order in  $g_x\Delta$ , the ratio  $\nu_f/\nu_h = (\gamma_f/\gamma_h)(1 - g_x\Delta/B_0)$ , from whence we establish that  $\Delta \approx 0.0085 \text{ cm}$ . Estimates of the effects of thermodiffusion (presented in the Supplemental Material [13]) are roughly consistent with the measured gradients. The rms drift in the ratio  $\nu_f/\nu_h$  shown in Fig. 2(b) is about  $3 \times 10^{-5}$ . This would be accounted for by gradient drift of about  $3 \mu\text{G}/\text{cm}$ . Given that the sample is being shuttled up and down, such gradient drift does not seem unreasonable.

The ultimate sensitivity of precision measurements based on a thermally polarized pentane-HFB sample can be estimated as follows: The accuracy with which one can determine the precession frequency of species  $j$  in a single measurement of duration  $T_2$  is  $\delta\nu_j \approx \rho/(2\pi B_j T_2^{3/2})$ , where  $\rho$  is the magnetometer sensitivity and  $B_j$  is the magnitude of the magnetic field due to species  $j$ . If the distance from the sensor to the sample is equal to twice the sample radius, the signal amplitude is  $B_j = \pi M_j/3$ , where the magnetization due to species  $j$  is  $M_j = n_j \mu_j^2 B_p/kT$ . Here  $n_j$  is the density of species  $j$ ,  $\mu_j$  its magnetic moment, and  $B_p$  is the polarizing field. In an equal-volume mixture of pentane and HFB, the  $^1\text{H}$  and  $^{19}\text{F}$

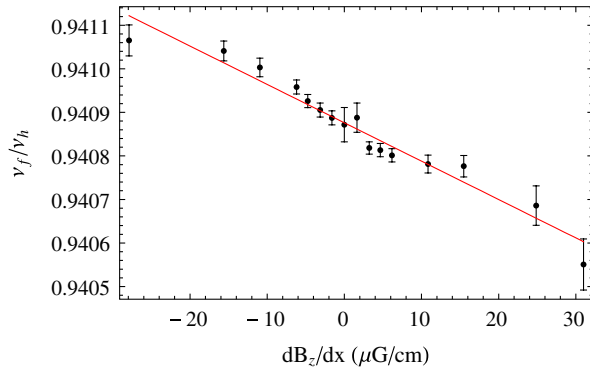


FIG. 3 (color online). Effects of gradients on the pentane-HFB comagnetometer. A gradient  $dB_z/dx$  was applied and the ratio  $\nu_f/\nu_h$  is plotted. The variation in the ratio of the frequencies indicates that there is some separation of the two solvents.

densities are  $n_h = 3.1 \times 10^{22} \text{ cm}^{-3}$  and  $n_f = 1.6 \times 10^{22} \text{ cm}^{-3}$ . For  $B_p = 100 \text{ kG}$  and  $T = 300 \text{ K}$ ,  $B_{h,f} = 16$  and  $7 \text{ } \mu\text{G}$  for  $^1\text{H}$  and  $^{19}\text{F}$ , respectively. (We verified that signal amplitudes in the present experiment are roughly consistent with those expected from thermal polarization; see the Supplemental Material [13].) SQUIDs and atomic magnetometers are both capable of reaching sensitivities below  $10 \text{ pG/Hz}^{1/2}$ . Using these numbers, and  $T_2 = 10 \text{ s}$ , we find that the single-shot frequency resolution is about  $\delta\nu = 3 \times 10^{-9}$  and  $7 \times 10^{-9} \text{ Hz}$  for  $^1\text{H}$  and  $^{19}\text{F}$ , respectively. Averaging  $10^4$  such measurements for a total integration time of roughly 1 day improves these numbers by a factor of 100. Spin-projection noise of the nuclei is several orders of magnitude smaller than that imposed by the finite sensitivity of the magnetometers, leaving considerable room for improvement.

Frequency resolution of  $3 \times 10^{-9} \text{ Hz}$  for protons in a 10 s measurement corresponds to magnetic-field sensitivity of about  $1.5 \text{ pG}/\sqrt{\text{Hz}}$ , approaching the sensitivity of the state-of-the-art SQUID and alkali-vapor atomic magnetometers.

One can envision many alternative liquid-state comagnetometer schemes and we briefly present one based on a mixture of hyperpolarized  $^{129}\text{Xe}$  and pentane. Xenon is attractive for such an application because it has a very long transverse relaxation time and hyperpolarization boosts signal considerably. In the pentane-xenon mixture, protons are polarized via the spin-polarization induced nuclear Overhauser effect [16,17], eliminating the need for a pre-polarizing magnet. Furthermore, xenon  $T_1$  is so long ( $\approx 400 \text{ s}$  for the conditions of measurements presented here) that many transients can be acquired in a single batch of hyperpolarized xenon. An ultralow-field NMR signal of a mixture of hyperpolarized liquid  $^{129}\text{Xe}$  and pentane is presented in Fig. 4. These data were acquired following a  $\pi/2$  pulse, resonant with the proton Larmor precession frequency. This pulse also produced a small transverse excitation of the  $^{129}\text{Xe}$  spins, tipping them into the

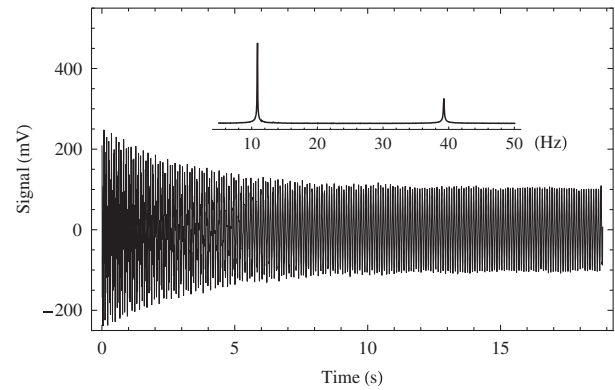


FIG. 4. Ultralow-field NMR signals obtained in a mixture of hyperpolarized liquid xenon and pentane. These data were acquired with SQUID magnetometers in a 10 mG magnetic field. The inset shows the magnitude Fourier transform.

transverse plane by about  $1^\circ$ – $2^\circ$ . Spin precession was monitored by SQUID magnetometers in a 10 mG, magnetically shielded environment. The inset shows the magnitude Fourier transform, with the proton signal at 39 Hz and the  $^{129}\text{Xe}$  signal at 10.5 Hz. Proton  $T_2$  was about 3.2 s for these data.  $T_2$  for xenon was too long to be accurately measured by this data set, although we estimate it to be about 250 s. More details of the apparatus used for these measurements can be found in Refs. [17,18].

We now discuss several possible applications for such liquid-state comagnetometers.

*Precision measurements of spin gravity.*—There has been both experimental [1,19–22] and theoretical [23,24] interest in the question of whether spins can couple to gravity. Such an interaction violates invariance under time reversal ( $T$ ), equivalent to  $CP$ , the combined symmetries of charge conjugation ( $C$ ) and spatial inversion ( $P$ ). The exchange of hypothetical pseudoscalar particles [25], such as axions, with an unpolarized massive body (e.g., Earth) would lead to similar effects. The  $^1\text{H}$ – $^{19}\text{F}$  comagnetometer outlined here could be employed for such tests by configuring the apparatus so that the Earth’s gravitational acceleration  $\mathbf{g}$  has a nonzero projection along the magnetic field. In the presence of a spin-gravity coupling, the ratio of precession frequencies would be different depending on the orientation of the magnetic field. The presently considered comagnetometer has an advantage over the  $^{199}\text{Hg}$ – $^{201}\text{Hg}$  comagnetometer of Ref. [1] in that both protons and  $^{19}\text{F}$  nuclei are spin-1/2 particles. In the case of  $^{201}\text{Hg}$ , with nuclear spin  $I = 3/2$ , interaction of the nuclear quadrupole moment with the cell walls can result in systematic effects. Reaching sensitivity of  $10^{-11} \text{ Hz}$  would represent about four orders of magnitude improvement over the limits of Ref. [1]. Since the  $^{19}\text{F}$  nucleus has an unpaired neutron, the experiment would be sensitive to a spin-gravity coupling with a linear combination of proton and neutron spin.

*Permanent EDMs.*—A permanent EDM of an atom or an elementary particle also violates invariance under  $T$  and  $CP$ , and has long been hailed as an unambiguous signature of new physics beyond the standard model. Present experimental limits on the EDM of the electron [3], neutron [26], and  $^{199}\text{Hg}$  atom [4] have placed constraints on many proposed extensions to the standard model [27]. The  $^1\text{H}$ – $^{129}\text{Xe}$  comagnetometer scheme outlined here could be used for such an experiment by applying an electric field either parallel or antiparallel to the magnetic field. An EDM interacts with an electric field via  $H_{\text{EDM}} = d_s^{\frac{\hbar}{e}} \cdot \mathbf{E}$ . Reversal of  $\mathbf{E}$  gives rise to a frequency shift  $\delta\nu_{\text{Xe}} = 4dE/h$ .  $CP$  violating effects are strongly enhanced in heavy nuclei, so the proton-precession frequency would be used to compensate for magnetic field fluctuations. In addition to previously mentioned attributes, liquid xenon is appealing for this application because it has a very high electric field breakdown strength, on the order of 400 kV/cm [28], and the hydrocarbons we discuss here also have high electric field breakdown strength. With  $E = 400$  kV/cm, frequency resolution of  $4 \times 10^{-11}$  Hz corresponds to an EDM limit of approximately  $1.3 \times 10^{-31} e \cdot \text{cm}$ . This is roughly two orders of magnitude better than the  $1.3 \times 10^{-29} e \cdot \text{cm}$  statistical sensitivity of the  $^{199}\text{Hg}$  EDM experiment of Ref. [4], and four orders of magnitude better than the limit set by a gas-phase  $^3\text{He}$ – $^{129}\text{Xe}$  comagnetometer [2], each obtained over months of integration.

*Gyroscopes.*—Since the spins define an inertial reference frame, they can be used to sense rotations. Sensitivity to rotations at the level of  $5 \times 10^{-9}$  Hz in a single 10 s measurement would form a gyroscope competitive with other technologies based on cold atoms, ring lasers, and overlapping ensembles of electron and nuclear spins [29].

Finally, we briefly address the effects of dipolar fields. In liquid state, local dipolar fields are rapidly averaged to zero on account of diffusion; however, long-range dipolar fields are not averaged to zero and may influence spin precession. Spin evolution in such fields can lead to linear (associated with sample shape [18,30]) and nonlinear (associated with magnetic field or magnetization gradients [31]) effects, characterized by a time scale  $\approx \gamma M$ . For HFB–pentane mixture, thermally polarized in a 10 T field, this is on the order of  $0.1 \text{ s}^{-1}$  for either species. Mixtures involving hyperpolarized liquid xenon will exhibit much stronger dipolar fields. Thus, care will have to be taken to mitigate the effects of dipolar fields. Linear effects can be suppressed by employing a spherical sample cell, and nonlinear effects involving magnetic field or magnetization gradients may be reduced by active mixing. The presence of two spin species will enable compensation of noise due to linear frequency shifts associated with cell deformations in the same way it enables compensation due to external magnetic field fluctuations.

It is worth putting some of these considerations in the context of an earlier proposal to perform an EDM experiment neat liquid  $^{129}\text{Xe}$  [31]. This experiment was complicated by nonlinear effects due to long-range dipolar fields when the spins are tipped into the transverse direction by  $90^\circ$ . These nonlinear effects are highly suppressed if the spins are tipped by only a few degrees [32]; however, this precludes operation in the gradiometer mode suggested in Ref. [31]. The presence of a second nuclear spin species would allow one to operate in the small tip angle regime, while retaining a second channel to compensate for magnetic field or magnetization fluctuations.

In conclusion, we have demonstrated operation of liquid-state nuclear-spin comagnetometers based on mixtures of mutually miscible solvents, each rich in a different spin species. We have outlined how such a device could be used for precision measurements such as a test of spin-gravity coupling and a search for permanent EDMs. Estimates based on signal-to-noise ratio for realistic conditions indicate that such devices may be two to four orders of magnitude more sensitive than previous experiments.

This research was supported by the National Science Foundation under Award No. CHE-0957655 (D.B. and M.P.L.), by the U.S. Department of Energy, Office of Basic Energy Sciences, Division of Materials Sciences and Engineering under Contract No. DE-AC02-05CH11231 (J.W.B. and A.P.), and by the Kolumb program of the Foundation for Polish Science (S.P.). We thank S. Knappe and J. Kitching for supplying the microfabricated alkali vapor cell.

---

\*micah.ledbetter@gmail.com

- [1] B.J. Venema, P.K. Majumder, S.K. Lamoreaux, B.R. Heckel, and E.N. Fortson, *Phys. Rev. Lett.* **68**, 135 (1992).
- [2] M.A. Rosenberry and T.E. Chupp, *Phys. Rev. Lett.* **86**, 22 (2001).
- [3] B.C. Regan, E.D. Commins, C.J. Schmidt, and D. DeMille, *Phys. Rev. Lett.* **88**, 071805 (2002).
- [4] W.C. Griffith, M.D. Swallows, T.H. Loftus, M.V. Romalis, B.R. Heckel, and E.N. Fortson, *Phys. Rev. Lett.* **102**, 101601 (2009).
- [5] D. Bear, R.E. Stoner, R.L. Walsworth, V.A. Kostelecký, and C.D. Lane, *Phys. Rev. Lett.* **85**, 5038 (2000).
- [6] C. Gemmel *et al.*, *Eur. Phys. J. D* **57**, 303 (2010).
- [7] M. Smiciklas, J.M. Brown, L.W. Cheuk, S.J. Smullin, and M.V. Romalis, *Phys. Rev. Lett.* **107**, 171604 (2011).
- [8] T.W. Kornack, R.K. Ghosh, and M.V. Romalis, *Phys. Rev. Lett.* **95**, 230801 (2005).
- [9] See comments by M. Packard and R. Varian in J. Kaplan, *Phys. Rev.* **93**, 939 (1954).
- [10] G.S. Waters and P.D. Francis, *J. Sci. Instrum.* **35**, 88 (1958).
- [11] W.F. Stuart, *Rep. Prog. Phys.* **35**, 803 (1972).
- [12] M.P. Ledbetter, T. Theis, J.W. Blanchard, H. Ring, P. Ganssle, S. Appelt, B. Blümich, A. Pines, and D. Budker, *Phys. Rev. Lett.* **107**, 107601 (2011).

- [13] See Supplemental Material at <http://link.aps.org/supplemental/10.1103/PhysRevLett.108.243001> for additional details of the experimental setup, signal amplitude and phase, and additional ultra-low-field NMR signals.
- [14] C. R. Patrick and G. S. Prosser, *Nature (London)* **187**, 1021 (1960).
- [15] *Handbook of Chemistry and Physics*, edited by R. C. Weast, M. J. Astle, and W. H. Beyer (CRC Press, Boca Raton, FL, 1985), 66th ed.
- [16] G. Navon, Y.-Q. Song, T. Room, S. Appelt, R. E. Taylor, and A. Pines, *Science* **271**, 1848 (1996).
- [17] J. J. Heckman, M. P. Ledbetter, and M. V. Romalis, *Phys. Rev. Lett.* **91**, 067601 (2003).
- [18] M. P. Ledbetter, G. Saielli, A. Bagno, N. Tran, and M. V. Romalis, [arXiv:1112.5644](https://arxiv.org/abs/1112.5644).
- [19] B. R. Heckel *et al.*, *Phys. Rev. D* **78**, 092006 (2008).
- [20] D. J. Wineland and N. F. Ramsey, *Phys. Rev. A* **5**, 821 (1972).
- [21] D. J. Wineland, J. J. Bollinger, D. J. Heinzen, W. M. Itano, and M. G. Raizen, *Phys. Rev. Lett.* **67**, 1735 (1991).
- [22] D. F. Jackson Kimball, L. R. Jacome, S. Guttikonda, E. J. Bahr, and L. F. Chan, *J. Appl. Phys.* **106**, 063113 (2009).
- [23] J. Leitner and S. Okubo, *Phys. Rev.* **136**, B1542 (1964); N. D. Hari Dass, *Phys. Rev. Lett.* **36**, 393 (1976); W. T. Ni, *Phys. Rev. Lett.* **38**, 301 (1977).
- [24] Victor Flambaum, Simon Lambert, and Maxim Pospelov, *Phys. Rev. D* **80**, 105021 (2009).
- [25] J. E. Moody and F. Wilczek, *Phys. Rev. D* **30**, 130 (1984).
- [26] C. A. Baker *et al.*, *Phys. Rev. Lett.* **97**, 131801 (2006).
- [27] M. Pospelov and A. Ritz, *Ann. Phys. (N.Y.)* **318**, 119 (2005).
- [28] S. E. Derenzo, T. S. Mast, H. Zaklad, and R. A. Muller, *Phys. Rev. A* **9**, 2582 (1974).
- [29] C. Jentsch, T. Müller, E. M. Rasel, and W. Ertmer, *Gen. Relativ. Gravit.* **36**, 2197 (2004); S. J. Sanders, L. K. Strandjord, and D. Mead, in *15th Optical Fiber Sensors Conference*, Technical Digest (IEEE, Portland, 2002), p. 5; G. E. Stedman, K. U. Schreiber, and H. R. Bilger, *Classical Quantum Gravity* **20**, 2527 (2003); T. L. Gustavson, A. Landragin, and M. A. Kasevich, *Classical Quantum Gravity* **17**, 2385 (2000); T. W. Kornack, R. K. Ghosh, and M. V. Romalis, *Phys. Rev. Lett.* **95**, 230801 (2005).
- [30] M. Goldman and H. Desvaux, *Chem. Phys. Lett.* **256**, 497 (1996).
- [31] M. V. Romalis and M. P. Ledbetter, *Phys. Rev. Lett.* **87**, 067601 (2001).
- [32] M. P. Ledbetter and M. V. Romalis, *Phys. Rev. Lett.* **89**, 287601 (2002).